Available online at www.sciencedirect.com
ScienceDirect
International Journal of Heat and Mass Transfer 51 (2008) 2411–2417
International Journal of HEAT and MASS TRANSFER
www.elsevier.com/locate/ijhmt

Investigation on the effects of fly ash particles on the thermal radiation in biomass fired boilers

M. Bahador, B. Sundén *

Division of Heat Transfer, Department of Energy Sciences, Lund University, Box 118, S-221 00 Lund, Sweden

Received 8 February 2007
Available online 17 October 2007

Abstract

Ash is produced in combustion of biomass. Some part of this matter is called fly ash and is carried by the flow and causes not only air pollution and erosion, but also can affect the thermal radiation. The effects of fly ash particles on the thermal radiation are considered in this investigation. By analyzing sampled data in an electrostatic filter, a realistic particle size distribution is found. Although the optical data on biomass fly ash are not available, however, similarity between coal and biomass ash compositions showed that the optical constants of the low Fe coal fly ash can be applied for the biomass fly ash. The Mie theory is used to predict scattering and absorption coefficients and phase function. The mean Planck scattering and absorption coefficients and phase function are predicted by averaging over the particle size distribution and Planck function, respectively. The effects of fly ash particles on thermal radiation are evaluated by a three-dimensional test case. It is assumed that the medium is a mixture of non-grey gases and different level of particle loading. Predicted results from the test case showed that the fly ash can be influential on the thermal radiation. In addition, in selected fly ash volume fractions, the effect of scattering by particles is not so important on the radiative heat source and radiative heat flux to the wall whereas their absorption effect is important and can increase the radiative heat source and wall heat fluxes.

Keywords: Thermal radiation; Mie scattering theory; Fly ash; Particle size distribution; Finite volume method; Non-grey radiation

1. Introduction

Thermal radiation is the dominate heat transfer mode in boilers. Using fuels such as coal or biomass in boilers produces particles which absorb, emit and anisotropically scatter the thermal radiation. Radiative properties of these particles are strongly depending on their composition and size. This study predicts radiative properties of particles and evaluates their effects on thermal radiation in biomass fired boilers. Earlier studies have shown that the radiative heat transfer is the dominating heat transfer mode in coal furnaces. In such furnaces, coal, char and fly ash particles absorb, emit and anisotropically scatter thermal radiation and their radiative properties are affected by their composition and size. Previously, the radiation scattering in coal furnaces has been studied by Gupta et al. [1]. In their study the Planck scattering and absorption coefficients were calculated by the Mie theory. An exponential particle size distribution, isotropic and anisotropic phase functions were studied with the Monte Carlo method. Their study showed that the heat transfer is overestimated because of neglecting scattering. The radiative properties of fly ash in coal-fired systems for two different particle size distributions have been studied by Goodwin and Mitchner [2]. In their research, scattering and absorption coefficients were calculated by using the Mie theory and spectral optical constants. In a similar work, Liu and Swithenbank [3] used a simplified Mie theory and calculated the spectral and Planck scattering and absorption coefficients. In another study by Marakis et al. [4], the absorption and scattering of particles were evaluated in a cylindrical coal fired furnace. The radiative properties were calculated by using the Mie theory and spectral optical constants for coal, char

* Corresponding author. Tel.: +46 462228605; fax: +46 462224717.
E-mail address: Bengt.Sunden@vok.lth.se (B. Sundén).

0017-9310/$ - see front matter © 2007 Elsevier Ltd. All rights reserved.
doi:10.1016/j.ijheatmasstransfer.2007.08.013

Nomenclature

c	distance between particles
D	particle diameter
f_v	particle volume fraction
I	intensity
k	optical constant (imaginary part)
m	optical constant
N	series number
Q	efficiency
r	position vector
S	direction vector
x	size parameter

Greek symbols

θ	scattering angle
κ	absorption coefficient
λ	wavelength
μ	mean of data
ρ	density
σ	scattering coefficient
σ_1	standard deviation of data
Φ	phase function
Ω	solid angle

Subscripts

A	absorption
b	blackbody
D	diameter
λ	spectral
P	mean Planck
t	total
s	scattering

and fly ash particles. A gamma particle size distribution was applied on clouds of non-uniform particles. In their study, $P-1$ and Monte Carlo methods were compared and the results showed that particles have significant effect on the wall heat fluxes. Combustion of biomass produces particles which are very similar to those of coal combustion. Soot, fly ash and char are main particles in the biomass combustion. From the composition viewpoint, soot and char consist of mainly carbon whereas fly ash consists of refractory components such as CaO, MgO, SiO_2 and the radiative properties become strongly dependent on the wavelength. From size viewpoint, in biomass combustion, the soot particles are in the range of some nm [5] while the char particles are large particles with sizes about some hundred μm [6]. However, the size of fly ash particles varies in a large range from nm up to some hundred μm. The objective of the present study is to predict the scattering and absorption coefficients of the fly ash and evaluate its effects on the radiative heat transfer in biomass boiler. Similar to previous studies some data for optical properties and size distributions of fly ash are needed. The Mie scattering theory is applied to predict particle scattering and absorption coefficients and phase function. The data are used to solve the radiative transfer equation (RTE) in a three-dimensional rectangular geometry to evaluate the effects of particles on overall radiative heat transfer inside a boiler.

2. Formulation

2.1. Scattering of the thermal radiation by particles

The interaction of electromagnetic waves and particles can change the direction and amount of energy which is carried by the waves. Although for scattering problems there are some boundary solutions available such as Rayleigh, Rayleigh Gans and so on, however, when the particle diameter varies widely and most of the particle abundance is focused in several micrometers, the Mie scattering theory will be the most suitable method for study of particle scattering. This analytical method, analyses the interaction of a single spherical particle and electromagnetic waves and its details can be found in van de Hulst [7], Kerker [8] and Bohren and Huffman [9]. The Mie computations are relatively straightforward although in some rare cases for instance, a partly absorbing sphere, numerical instability has been reported [10]. The necessary parameters for the Mie calculations are the size parameter ($x = \pi D/\lambda$) and optical constant ($m = n - ik$). The results of the Mie theory will be scattering and absorption efficiency factors, phase function and asymmetry factor as functions of size parameter. Here, for calculation of the mentioned parameters, a code from Bohren and Huffman [9] with the number of $N = x + 4x^{1/3} + 2$ for evaluation of infinite series is applied.

2.2. The fly ash optical constants

In biomass combustion, it can be assumed that the fly ash particles are formed from components such as SiO_2, Al_2O_3, Fe_2O_3, CaO and MgO [11]. Although this assumption may not be completely true for very fine fly ash particles and very coarse particles it may be good in the influential range on thermal radiation. Comparison between compositions in biomass and coal fly ashes reveals a close similarity in the types and amounts of the above mentioned mineral materials. An analysis of mineral components and their influence on optical constants for different type of coal fly ashes has been investigated by Im and Ahluwalia [12] and the general results are shown in Table 1.

As it is seen the most influential components on both scattering and absorption coefficient are common with

Table 1
Composition dependence of ash optical constants [12]

Wavelength (μm)	Refractive index, n	Absorption index, k
1–4	Mixture rule for SiO_2, CaO, Fe_2O_3 and MgO	$f(Fe^{2+}, Fe^{3+})$
4–8	Mixture rule for SiO_2, CaO, Fe_2O_3 and MgO	Silica glass data
8–13	SiO_2 Reststrahlen band, Al_2O_3 and MgO Reststrahlen Bands	Al_2O_3 and MgO Reststrahlen bands

the biomass fly ash. Here, due to the composition similarity, it is assumed that the optical constants data for the coal fly ash is applicable for the biomass fly ash. Therefore, in this study, available experimental optical constants data for the low Fe coal fly ash provided by Goodwin and Mitchner [2] is applied for the biomass fly ash. In order to simplify the application of these data in a numerical simulation, linear functions are fitted to them as given in Table 2.

2.3. Treatment of particle cloud

In the independent scattering regime ($c/\lambda \gg 1$), the spectral scattering coefficient in a uniform cloud of particles, is given by:

$$\sigma_\lambda = \frac{3 f_v Q_s}{2D} \tag{1}$$

where D and f_v are particle diameter and volume fraction, respectively, and Q_s is the scattering efficiency for the size distribution x. A similar equation is written for the spectral absorption coefficient. Assumption of the uniform particle cloud can be applied for all situations. For instance, fly ash particles vary in a large range from some nm up to some hundred μm. In such a situation, by using particle size distribution (PSD) the effect of non-uniformity of particles can be taken into account. In a biomass boiler, accurate prediction of PSD may depend on different parameters and it can also vary locally. In this study, for a realistic assumption, PSD is estimated by collected fly ash in an electrostatic filter. These data have been presented in Table 3.

Table 2
Models for the optical constants of fly ash

Optical constants		Range (μm)
n_λ	1.5	$\lambda < 3.4$
	$1.5 - 0.074(\lambda - 3.4)$	$3.4 \leqslant \lambda < 7.2$
	$1.22 - 0.46(\lambda - 7.2)$	$7.2 \leqslant \lambda < 8.2$
	$0.76 + 0.57(\lambda - 8.2)$	$8.2 \leqslant \lambda < 11$
	$2.3 - 0.56(\lambda - 11)$	$\lambda \geqslant 11$
k_λ	$10^{-2.96-4.6(\lambda-0.22)}$	$0.2 \leqslant \lambda < 0.5$
	$10^{-4.48+1.96(\lambda-0.5)}$	$0.5 \leqslant \lambda < 1$
	$10^{-3.5}$	$1 \leqslant \lambda < 4$
	$10^{-3.5+(\lambda-4)}$	$4 \leqslant \lambda < 5$
	$10^{-2.5+0.26(\lambda-5)}$	$5 \leqslant \lambda < 7.5$
	$10^{-1.86+1.76(\lambda-7.5)}$	$7.5 \leqslant \lambda < 8.5$
	$10^{-0.1}$	$8.5 \leqslant \lambda < 10.5$
	$10^{-0.1-1.0(\lambda-10.5)}$	$\lambda \geqslant 10.5$

Table 3
Size distribution analysis in vol. % on collected fly ash in an electrostatic filter

Low (μm)	High (μm)	Result in (%)	Low (μm)	High (μm)	Result in (%)
0.2	0.48	0.15	8.48	10.27	7.46
0.48	0.59	0.6	10.27	12.43	8.44
0.59	0.71	0.91	12.43	15.05	9.08
0.71	0.86	1.03	15.05	18.21	9.06
0.86	1.04	0.95	18.21	22.04	8.3
1.04	1.26	0.76	22.04	26.68	7.01
1.26	1.52	0.59	26.68	32.29	5.55
1.52	1.84	0.58	32.29	39.08	4.21
1.84	2.23	0.79	39.08	47.3	3.03
2.23	2.7	1.21	47.3	57.25	2.12
2.7	3.27	1.72	57.25	69.3	1.49
3.27	3.95	2.37	69.3	83.87	1.1
3.95	4.79	3.21	83.87	101.52	0.85
4.79	5.79	4.19	101.52	122.52	0.68
5.79	7.01	5.28	122.52	148.72	0.54
7.01	8.48	6.37	148.72	180	0.4

Statistical analysis of the data shows that the fly ash PSD consists of two distinguishable peaks in the sub and super micron regions and it can be represented by a heterogeneous log-normal distribution in the following form:

$$f(D) = \frac{w_1}{\sqrt{2\pi} D \sigma_{l,1}} e^{-\frac{(D-\mu_{l,1})^2}{2\sigma_{l,1}^2}} + \frac{w_2}{\sqrt{2\pi} D \sigma_{l,2}} e^{-\frac{(D-\mu_{l,2})^2}{2\sigma_{l,2}^2}} \tag{2}$$

where in this equation the values of the parameters are given as:

$$w_1 = 0.056, \quad w_2 = 0.944$$
$$\mu_{l,1} = -0.1193, \quad \mu_{l,2} = 2.655$$
$$\sigma_{l,1} = 0.3867, \quad \sigma_{l,2} = 0.8354$$

The heterogeneous log-normal model is fitted to the data and is presented in Fig. 1.

The spectral scattering and absorption coefficients and phase function in the non-uniform cloud of fly ash are pre-

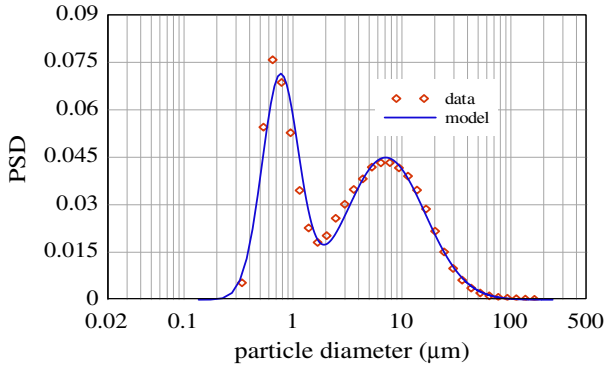

Fig. 1. Measured and modeled heterogeneous log-normal fly ash size distributions.

dicted by integration over the particle diameter using the PSD as [13]

$$\sigma_\lambda = 1.5 f_v \frac{\int_0^\infty Q_s D^2 f(D)\mathrm{d}D}{\int_0^\infty D^3 f(D)\mathrm{d}D} \tag{3}$$

$$\kappa_\lambda = 1.5 f_v \frac{\int_0^\infty Q_a D^2 f(D)\mathrm{d}D}{\int_0^\infty D^3 f(D)\mathrm{d}D} \tag{4}$$

$$\Phi_\lambda(\theta) = \frac{\int_0^\infty Q_s \Phi_{\lambda,D}(\theta) D^2 f(D)\mathrm{d}D}{\int_0^\infty Q_s D^2 f(D)\mathrm{d}D} \tag{5}$$

These equations show that the spectral scattering and absorption coefficients are linearly proportional to the fly ash volume fraction. The mean Planck scattering and absorption coefficients and total phase function are predicted by averaging the spectral results over the Planck function given by Eqs. (6)–(8).

$$\sigma_p = \int_0^\infty \sigma_\lambda I_{b\lambda}\mathrm{d}\lambda \Big/ \int_0^\infty I_{b\lambda}\mathrm{d}\lambda \tag{6}$$

$$\kappa_p = \int_0^\infty \kappa_\lambda I_{b\lambda}\mathrm{d}\lambda \Big/ \int_0^\infty I_{b\lambda}\mathrm{d}\lambda \tag{7}$$

$$\Phi(\theta) = \int_0^\infty \sigma_\lambda \Phi_{i,\lambda}(\theta) I_{b\lambda}\mathrm{d}\lambda \Big/ \int_0^\infty \sigma_\lambda I_{b\lambda}\mathrm{d}\lambda \tag{8}$$

3. Results

3.1. Radiative properties and phase function

Fig. 2 shows the variation of the mean Planck scattering and absorption coefficients of fly ash for $f_v = 1e{-}6$ of a uniform cloud of particles versus diameter. As can be seen, by increasing the temperature and decreasing the particle diameter (down to 1 μm), the mean Planck scattering coefficient increases and then sharply decreases whereas the mean Planck absorption coefficient decreases to a constant value.

In addition, Fig. 2 tells how important the size distribution of the particles is at different temperatures. A PSD, which focuses in the range of some μm, can have a large impact in calculations of both scattering and absorption coefficients. As can be seen, the fly ash inside of the range of 0.1–100 μm has a large scattering coefficient. In this study, the mentioned range is used as integration limits in Eqs. (3)–(5).

Results of the predicted radiative properties for some levels of fly ash volume fractions show that, for wavelengths below 8 μm the spectral scattering coefficient is strong whereas the values for spectral absorption coefficient are considerable for wavelengths above 8 μm (see Fig. 3).

Fig. 4 shows the mean Planck scattering and absorption coefficients. The mean Planck scattering coefficient at low temperature is smaller than at high temperature and increases with increasing temperature, because the peak of the Planck function at high temperature shifts to shorter wavelengths and for the same reason the mean Planck

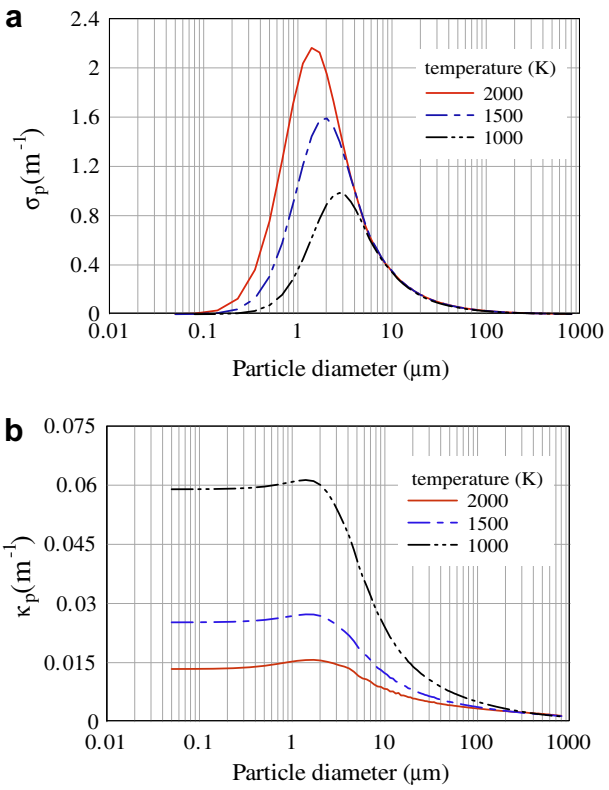

Fig. 2. Variation of mean Planck scattering (a) and absorption (b) coefficients versus diameter.

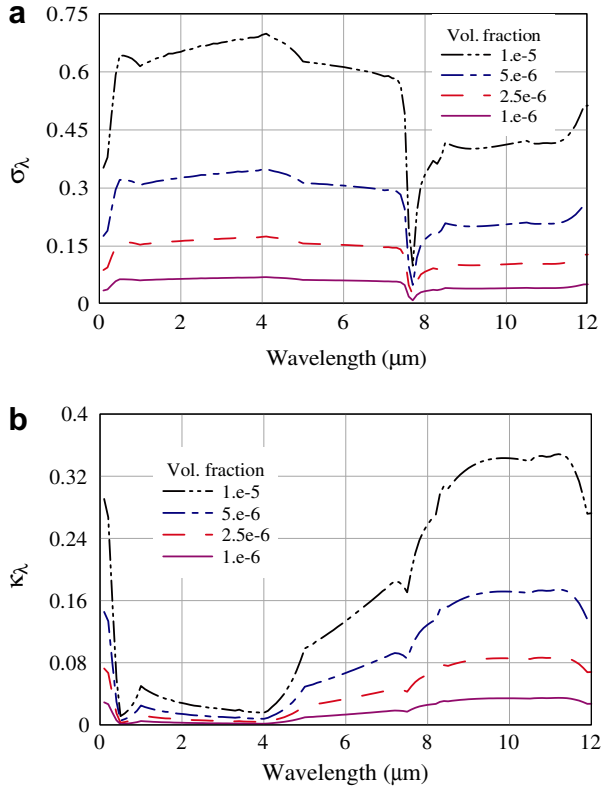

Fig. 3. Fly ash spectral scattering (a) and absorption (b) coefficients for different concentrations.

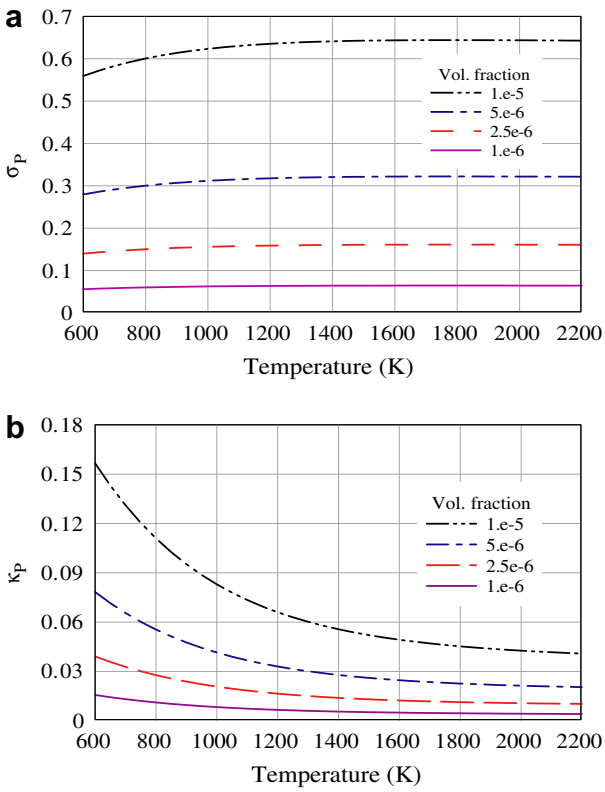

Fig. 4. Fly ash mean Planck scattering (a) and absorption (b) coefficients for different fly ash volume fraction.

absorption coefficient is large at low temperature. Both the scattering and absorption coefficients increase linearly by increasing the fly ash volume fraction. In this study, in order to apply temperature dependent values of the scattering and absorption coefficients, polynomial functions have been fitted to the data as shown in Table 4.

The average Mie phase function over particle diameter and Planck function is shown in Fig. 5 and it presents strong forward scattering and some backward scattering regimes.

3.2. Effects of fly ash on radiative heat transfer

In order to study the effect of fly ash on radiative heat transfer, a 3D rectangular enclosure with dimensions 2 m × 2 m × 4 m is considered. The temperature and emissivity for all the side walls are 498 K and 0.8, respectively. The bottom and top walls are at 1100 K and 800 K, respectively, and they are assumed to be black. The medium is assumed to be a mixture of 0.287 H_2O + 0.117 CO_2 and

Table 4
Polynomial coefficients fitted to the predicted data

$f(T)=a\left(\frac{T}{100}\right)^4+b\left(\frac{T}{100}\right)^3+c\left(\frac{T}{100}\right)^2+d\left(\frac{T}{100}\right)+e$					
$f(T)$ (m^{-1}/f_v)	a	b	c	d	e
σ_p	25755.4	8245.92	−670.487	24.592	−0.34278
κ_p	46219.8	−8100.43	621.96	−22.155	0.303024

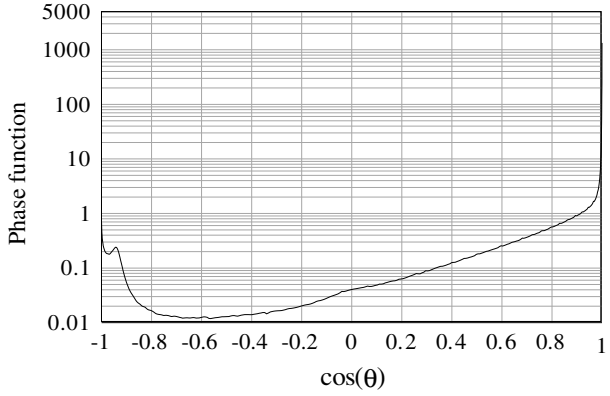

Fig. 5. Predicted phase function.

nitrogen (mole base). These values are average results which are predicted by modeling combustion in a fixed bed biomass boiler [14]. The gas temperature is non-uniform but symmetric around the centerline of the enclosure and is specified as $T=(T_c-T_e)f(r/R)+T_e$. In this equation, T_c is the gas temperature along the centerline of the enclosure and T_e is the exit temperature at $z=4$ m. Inside of the circular region of the cross section of the enclosure, the variation of the gas temperature is defined by $f(r/R)=(1-(r/R)^2)^{0.5}$, where r is the distance from the enclosure centerline and $R=1.4$ m is the radius of the centerline region. The gas temperature outside the circular region is assumed to be constant and equal to the exit temperature. The centerline temperature is assumed to increase linearly from 1100 K at the bottom of the enclosure ($z=0$ m) to 1600 K at $z=1$ m and then decrease linearly to 800 K at the exit. Different numerical methods are available for solution of the RTE. Jinbo et al. [15] have shown that in a medium with anisotropic scattering, reliable results are achieved by the finite volume method (FVM). In this study this methods is applied. Details of the procedure for discretization of the RTE in the FVM have been described in Chai et al. [16]. In addition the Mie phase function is applied in a similar approach as that introduced by Chai and Patankar [17]. In this approach the main control angles, $\Delta\ \Omega^l$and $\Delta\Omega^{l'}$, are divided into some sub-control angles and the average value of the phase function over all sub-control angles is predicted as:

$$\bar{\Phi}^{ll'}=\frac{\sum_{l_s=1}^{L_s}\sum_{l'_s=1}^{L'_s}\Phi^{l'_s l_s}\Delta\Omega^{l'_s}\Delta\Omega^{l_s}}{\Delta\Omega^{l'_s}\Delta\Omega^{l_s}} \tag{9}$$

For simulation of non-grey radiation of the mixture of H_2O, CO_2 and particles, the spectral line weighted sum of grey gases model (SLW) introduced by Denison and Webb [18] is applied. In this model, the RTE for an absorbing, emitting and scattering mixture of H_2O, CO_2 and particles is written as follows:

$$\frac{dI_{jk}(r,\hat{s})}{ds}=-(\kappa_{jk}+\kappa_p+\sigma_p)I_{jk}(r,\hat{s})+(\kappa_{jk}+\kappa_p)a_{jk}I_b(r)+\frac{\sigma_p}{4\pi}\int_{4\pi}I_{jk}(r,\hat{s}')\bar{\Phi}(\hat{s}',\hat{s})d\Omega' \tag{10}$$

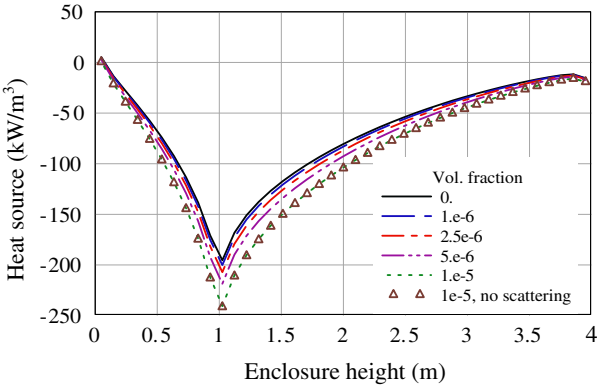

Fig. 6. Radiative heat source at the middle of the enclosure.

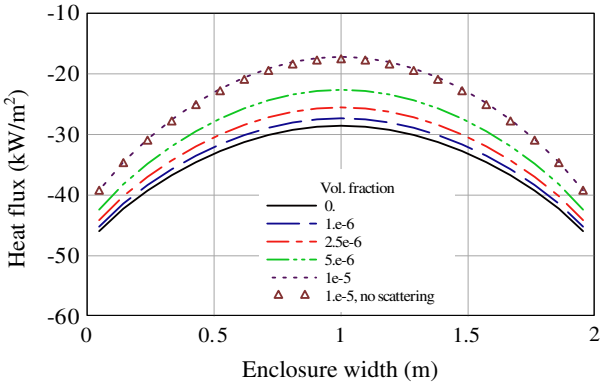

Fig. 8. Heat flux along the width of the enclosure.

where I_{jk} is the radiation intensity for the jth grey gas component of H_2O and kth grey gas component of CO_2. In addition, κ_p and σ_p are the mean Planck absorption and scattering coefficients of the particles. Details about application of this method in a mixture of H_2O and CO_2 can be found in [19]. The convolution approach with 20 logarithmically spaced absorption cross sections ranging from 1e−5 up to 100 is applied to give accurate result. For numerical solution of the RTE by the FVM the enclosure is divided into uniform $N_x \times N_y \times N_z = 21 \times 21 \times 41$ control volumes. In addition, in the cases with large values of fly ash volume fractions, different number of control angles was examined which showed that the uniform $N_\theta \times N_\varphi = 10 \times 12$ control angles and 5×5 sub-control angles (for phase function prediction), gave accurate results. The defined test cases in 0, 1e−6, 2.5e−6, 5e−6, 1e−5 levels of fly ash volume fractions are examined.

Fig. 6 shows the predicted radiative heat source along the centerline of the enclosure (1 m, 1 m, z). An increase in the fly ash volume fraction, increases the radiative heat source (regardless of the negative sign) and the highest increase is seen at $z = 1$ m. In addition, for selected levels of fly ash volume fraction, the absorption and emission of thermal radiation by particles seems to be influential and scattering has not an important role in the radiative heat source. However, increasing the volume fraction beyond 1e−5, which might be unrealistic, shows that scattering decreases the radiative heat source.

Fig. 7 shows predicted radiative heat flux along the height of the enclosure (0 m, 1 m, z). An increase in the fly ash volume fraction increases the radiative heat flux but absorption by the particles has a major role while the effect of scattering by the particles is not important.

Fig. 8 shows the predicted heat flux distribution along the width of the enclosure (x, 1 m, 0 m). It can be seen that the selected wall is radiating to the interior part of the enclosure and an increase in the fly ash volume fraction decreases the predicted heat flux.

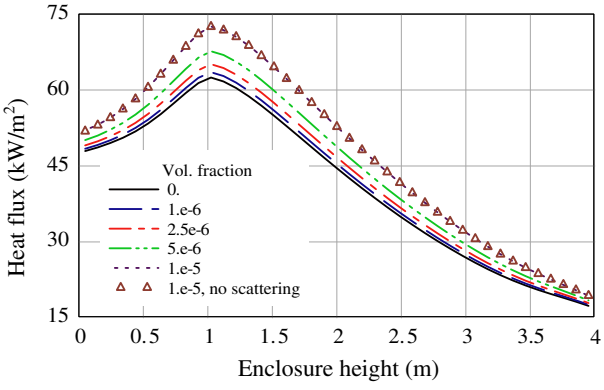

Fig. 7. Heat flux along the height of the enclosure.

4. Conclusions

Experimental data and realistic assumptions were used to predict the scattering and absorption properties of fly ash and its effects on the thermal radiation. By using analysis of a uniform particle cloud, the effects of PSD on predicted properties were discussed and it was found that the both scattering and absorption coefficients have considerable values in the range of some μm. The spectral and mean Planck scattering and absorption coefficients of fly ash were predicted. The results of mean Planck coefficients showed that an increase in the temperature increases the scattering coefficient whereas it decreases the absorption coefficient. In order to study the effect of fly ash on thermal radiation, a three-dimensional test case with non-grey gases was defined. Predicted results from the test case showed that by increasing the fly ash volume fraction, particles will be more influential on thermal radiation. However, the particle absorption plays a major role and the scattering of thermal radiation by particles at selected levels of the volume fraction is not important but further increase of the volume fraction decreases the radiative heat source and also the heat flux to the wall which may not be realistic.

Acknowledgements

The authors acknowledge the financial support by the Swedish National Scientific Council (VR) and the Combus-

tion Processes Competence Centre at Lund. In addition, the assistance of ALSTOM Company in Sweden by preparation of the particle size data is kindly appreciated.

References

[1] R.P. Gupta, T. F Wall, J.S. Truelove, Radiative scatter by fly ash in pulverized-coal-fired furnaces: application of the Monte Carlo method to anisotropic scatter, Int. J. Heat Mass Transfer 26 (1983) 1649–1660.
[2] D.G. Goodwin, M. Mitchner, Fly ash radiative properties and effects on radiative heat transfer in coal-fired systems, Int. J. Heat Mass Transfer 32 (1989) 627–638.
[3] F. Liu, J. Swithenbank, The effects of particle size distribution and refractive index on fly ash radiative properties using a simplified approach, Int. J. Heat Mass Transfer 36 (1996) 1905–1912.
[4] J.G. Marakis, C. Papapavlou, E. Kakaras, A parametric study of radiative heat transfer in pulverized coal combustion furnaces, Int. J. Heat Mass Transfer 43 (2000) 2961–2971.
[5] M. Strand, Particle formation and emission in moving grate boilers operation on woody biofuels, Ph.D. Thesis, Växjö University, No. 51, 2004.
[6] K. Bergqvist, Å. Myringer, D. Nordgren, S. Rydberg, Om förbränning av askor i rosterpannor, report 914, Värmeforsk company, 2004 (in Swedish).
[7] H.C. van de Hulst, Light Scattering by Small Particles, Chapman and Hall, London, 1975.
[8] M. Kerker, The Scattering of Light, Academic Press, New York, 1969.
[9] C.F. Bohren, D.R. Hoffman, Absorption and Scattering of Light by Small Particles, John Wiley & Sons, New York, 1998.
[10] A.L. Crosbie, G.W. Davidson, Dirac-delta function approximations to the scattering phase function, J. Quant. Spectrosc. Radiant. Transfer 33 (1985) 391–409.
[11] V.S. Loo, J. Koppejan, Handbook of Biomass Combustion and Co-firing, Twente University Press, 2003.
[12] K.H. Im, R.K. Ahluwalia, Radiation properties of coal combustion products, Int. J. Heat Mass Transfer 36 (1993) 293–302.
[13] L.A. Dombrovsky, Radiation Heat Transfer in Disperse System, Begell House, 1996.
[14] T.K. Nilsson, T. Klason, X.S. Bai, B. Sundén, Thermal radiation heat transfer and biomass combustion in a large-scale fixed bed boiler, ASME IMECE 2003-42249.
[15] H. Jinbo, R. Liming, T. Heping, Effects of anisotropic scattering on radiative heat transfer in two-dimensional rectangular media, J. Quant. Spectrosc. Radiant. Transfer 78 (2003) 151–161.
[16] J.C. Chai, H.S. Lee, S.V. Patankar, Finite volume method for radiation heat transfer, AIAA J. Thermophys. Heat Transfer 8 (3) (1994) 419–425.
[17] J.C. Chai, S.V. Patankar, Finite volume method for radiation heat transfer, in: Minkowycz and Sparrow (Ed.), Advances in Numerical Heat Transfer, vol. 2, 2000, pp. 109–138.
[18] M.K. Denison, B.W. Webb, The spectral line-based weighted-sum-of-gray-gases model in nonisothermal nonhomogeneous media, ASME J. Heat Transfer 117 (1995) 359–365.
[19] M.K. Denison, B.W. Webb, The spectral-line weighted-sum-of-gray-gases model for H_2O/CO_2 mixtures, ASME J. Heat Transfer 117 (1995) 788–792.